AIAA SciTech Forum
6-10 January 2025, Orlando, FL
AIAA SCITECH 2025 Forum

10.2514/6.2025-0014

Dual-Band Wavelength-Modulated Infrared Laser-Induced-Fluorescence Thermometry of CO

Jonathan O. Rustad *, Garrett C. Mathews†, and Christopher S. Goldenstein ‡
Purdue University, West Lafayette, IN 47907

This work presents a novel infrared dual-band wavelength-modulated laser-induced-fluorescence (WM-LIF) diagnostic to determine gas temperature via CO at a repetition rate of 10 Hz. This technique utilizes a quantum-cascade laser (QCL) emitting near 2013.3 cm^{-1} and a wavelength-tunable optical parametric oscillator (OPO) emitting near 4294.6 cm^{-1} to sequentially scan across the P(0,30) transition in the fundamental vibrational band of CO and the R(0,9) transition in the first overtone band of CO. Both lasers are scanned at 10 Hz and modulated at 5 kHz to generate background-free WM-LIF harmonic signals. A model describing the WM-LIF signals in the time and frequency domains was developed and least-squares fit to the measured WM-LIF first-harmonic $(1f)$ signal to extract the collisional-broadening full-width, integrated area, and characteristic times of the WM-LIF signal for each CO transition. The two color ratio of the integrated area from each laser was used to infer the temperature of CO in a heated jet and diffusion flame of 49/2/49 $CO/H_2/Ar$ at atmospheric pressure.

I. Nomenclature

A_{int}	=	integrated absorbance of an absorption transition
a_m	=	frequency modulation amplitude
E"	=	lower-state energy of an absorption transition
f_m	=	modulation frequency
FQY	=	fluorescence quantum yield
L	=	path length through imaged volume
P	=	optical power
p_0	=	normalized power-modulation amplitude
$\overline{P}$	=	nominal laser power
P_i	=	partial pressure of absorbing species
S	=	absorption transition linestrength
$S_{F,ss}$	=	steady state LIF signal
$S_{F,1f}$	=	first harmonic of the LIF signal
t	=	time
T	=	gas temperature
τ	=	characteristic time of LIF signal
τ_{decay}	=	characteristic decay time of LIF signal
τ_{ss}	=	characteristic time for LIF signal to reach steady state
α	=	spectral absorbance
η	=	collection efficiency
ν	=	optical frequency
$\overline{\nu}$	=	nominal optical frequency
ψ	=	phase shift between frequency and power modulation
ϕ	=	absorption transition lineshape

*Graduate Student, School of Aeronautics and Astronautics, 701 W Stadium Ave, West Lafayette, IN 47907.
†Former Postdoctoral Research Associate, School of Mechanical Engineering, 585 Purdue Mall, West Lafayette, IN 47907
Research Scientist, Mechanical Engineering, University of Colorado, Boulder, CO
‡Associate Professor, School of Mechanical Engineering, 585 Purdue Mall, West Lafayette, IN 47907, AIAA Associate Fellow.

II. Introduction

Infrared laser-induced fluorescence (IR-LIF) offers the potential to provide spatially resolved measurements of gas properties via many infrared active species. However, the technique has not been widely applied, in part, due to the lack of availability of high-power infrared light sources. Most previous work on IR-LIF has used pulsed lasers to image CO and CO_2 such as in the early work of Kirby and Hanson [1–3].

Recently, several continuous-wave (CW) wavelength-tunable infrared light sources with relatively high power have become available which facilitates the development of CW IR-LIF diagnostics. Goldenstein et al. developed an IR-LIF diagnostic using a quantum cascade laser for point measurements of temperature, pressure, and CO_2 mole fraction at ambient temperature with repetition rates up to 100 Hz [4]. In addition, Mathews and Goldenstein [5] developed the first wavelength-modulated infrared planar laser-induced-fluorescence diagnostic for background-free imaging of CO and demonstrated this in CO-H_2 diffusion flames. More recently, Mathews et al. [6] developed the first IR-LIF thermometer for combustion gases with a repetition rate of 1 kHz. That work employed a dual-band approach to scan across two CO transitions using a QCL near 4.9 μm and an OPO emitting near 2.3 μm.

This work builds on that done previously in our lab by Matthews et al. [5, 6] to develop the first WM-LIF thermometer. Again, a dual-band excitation scheme with a QCL and OPO was used to provide sensitive two-color thermometry. However, here we have expanded this method to perform WM-LIF in order to provide background-free measurements in hot gases with substantial spontaneous emission that is resonant with the IR-LIF signals. This represents an important stepping stone towards high-fidelity thermometry in combustion gases and other hot flows where the LIF signal is likely to be small compared to the background emission.

III. Theory

A. Laser-Induced Fluorescence

In LIF, laser light resonant with an absorption transition is used to pump molecules into an excited state where they can undergo spontaneous emission. In the weak excitation regime and steady state, the steady state LIF signal emitted from an optically thin volume, $S_{F,ss}$, is given by Eq. 1.

$$S_{F,ss}(\nu) = P(\nu) \times \alpha(\nu) \times \mathrm{FQY} \times \eta \tag{1}$$

Here, P is the laser power which depends on optical frequency ν, α is the spectral absorbance, FQY is the fluorescence quantum yield, and η is the fraction of emitted photons that are collected by the imaging system. The spectral absorbance is given by Eq. 2.

$$\alpha(\nu) = S(T) P_i \phi(\nu) L \tag{2}$$

Here, S is the transition linestrength, P_i is the partial pressure of the absorbing species, ϕ is the transition lineshape function and L is the length of the volume of gas from which LIF signal is collected.

After the steady state LIF signal has been calculated the time-dependent LIF signal can be determined following a similar procedure as in Mathews et al. [6]. The time dependent LIF signal at a generic moment in time denoted by i is given by Eq. 3

$$S_{F,i} = S_{F,i-1} + \frac{\mathrm{d}S_{F,i}}{\mathrm{d}t} \Delta t \tag{3}$$

Where Δt is the time step in the model dictated by the inverse of the oscilloscope sample rate and $\mathrm{d}S_{F,i}/\mathrm{d}t$ is given by Eq. 4

$$\frac{\mathrm{d}S_{F,i}}{\mathrm{d}t} = \frac{S_{F,ss,i-1} - S_{F,i-1}}{\tau} \tag{4}$$

Here τ is the characteristic LIF time where the value of τ can either be τ_{ss} or τ_{decay} depending on if the time-domain signal was less than or greater than the steady state signal, respectively.

B. Wavelength-Modulated LIF

In WM-LIF, the laser's wavelength and intensity are modulated at a high frequency to generate a modulated LIF signal with harmonic signals that are isolated from common noise sources (including background emission) in the frequency domain. As a result, WM-LIF offers several advantages, namely: (1) the measurements are background free and (2) have reduced noise. Both of which are particularly important for IR-LIF measurements in hot flows due to the large background emission and potentially small IR-LIF signal [5].

Injection current modulation of the light sources used here leads to intensity and frequency modulation [7] which are modeled as follows:

$$P(t) = \overline{P}[1 + p_0 \sin(2\pi f_m t)] \tag{5}$$

$$\nu(t) = \overline{\nu} + a_m \sin(2\pi f_m t + \psi) \tag{6}$$

Here $\overline{P}$ is the nominal laser power, p_0 is the normalized power-modulation amplitude, $\overline{\nu}$ is the nominal frequency of the laser, a_m is the frequency modulation depth (i.e., the modulation depth), and ψ is the phase shift between frequency and power modulation. The parameters p_0, $\overline{\nu}$, a_m, and ψ can be measured via the same techniques as described in [7]. Note: Eqs. 5 and 6 do not account for the contributions from the simultaneous injection-current scanning; but this was done as outlined in [7].

The harmonic signals embedded within $S_F(t)$ can be extracted using digital lock-in filters. In this work, a phase insensitive approach was taken where $S_f(t)$ is multiplied by a reference cosine and sine waves at the harmonic of interest to generate the X and Y signals respectively. The X and Y signal components are then low-pass filtered and the magnitude of a harmonic signal is given by the root-sum-square of the filtered $X(t)$ and $Y(t)$ components. For this work we used the first harmonic signal to infer temperature. The first harmonic of the WM-LIF signal is given by Eq. 7.

$$S_{F,1f}(t) = \sqrt{X_{1f}(t)^2 + Y_{1f}(t)^2} \tag{7}$$

IV. Experimental Procedures

A. Experimental Setup

Figure 1 shows a schematic of the experimental setup used to perform dual-band wavelength-modulated IR-LIF. The DFB seed laser of the OPO and the QCL were injection-current tuned with alternating ramp waveforms and modulated with a sine wave produced by an arbitrary function generator. This was done to scan the wavelength of each laser across an absorption transition of CO while simultaneously modulating the LIF signal to produce background-free harmonic signals ($1f$, $2f$, etc.). The light sources were scanned 180 degrees out of phase with each other to ensure that only one laser was scanning across a CO transition at a given time. The OPO seed laser and QCL were injection-current tuned with the ramp waveform at 10 Hz. To implement wavelength modulation, a sine wave was superimposed with a frequency of 5 kHz. The QCL was scanned across the P(0,30) transition of CO near 2013.3 cm^{-1} with an output power of 89 mW while the OPO scanned across the R(0,9) transition of CO near 4294.6 cm^{-1} with an optical power of approximately 2.5 W. These transitions were selected for two-color thermometry due to their large differences in lower state energies (E'' = 1783 cm^{-1} for the P(0,30) and E'' = 173.0 cm^{-1} for the R(0,9) transition). The higher power OPO was used to target the overtone transition while the much lower power QCL targeted a fundamental band transition. This scheme was chosen to yield similar magnitudes of LIF signals at relevant temperatures despite the significant differences in output power of the light sources.

The beams were combined using a dichroic mirror to yield a colinear beam across a heated jet or flame which contained a 49/2/49 mixture of $CO/H_2/Ar$ flowing at 2.2 m/s. A thermocouple was inserted into the steady flow prior to LIF measurements for comparison. The LIF signal was then collected and focused onto a LN_2 cooled InSb detector using a lens doublet which had two 25 mm focal length, 25.4 mm diameter CaF_2 lenses and, a 25.4 mm band-pass filter to attenuate background emission from the heated jet or flame. The InSb detector's voltage was recorded on a 16 bit Tektronix Oscilloscope at 1 MS/s. The intensity of the QCL and OPO were recorded with photodiode detectors to account for optical power variations across the wavelength scan, which alters the shape of the time-varying LIF signal. A germanium etalon was used to characterize the wavelength scanning and modulation of the QCL and OPO.

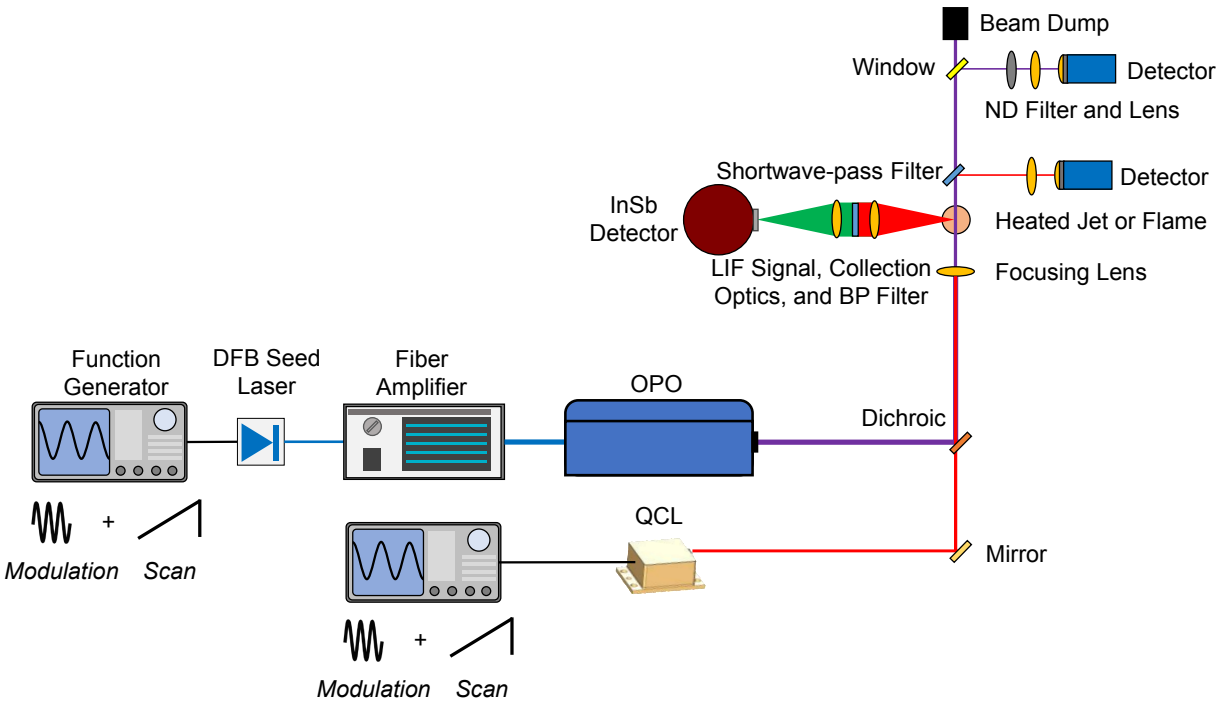

Fig. 1 Experimental setup used to perform WM-LIF temperature measurements of CO in a CO-H_2-Ar heated jet or flame at atmospheric pressure.

B. Data Processing

The measured WM-LIF signal was passed through a digital boxcar filter in the frequency domain to extract the first harmonic signal. A filter bandwidth of 260 Hz was selected to ensure sufficient filtering. The relative magnitude of integrated areas for each transition was determined using a nonlinear fitting routine to fit simulated first harmonic WM-LIF signals to the measured first harmonic WM-LIF signals. The WM-LIF signals were simulated in the frequency domain as a function of the characteristic LIF time (τ), integrated area (A_{int}), absorption linecenter frequency (ν_0), and collisional-broadening full-width at half maximum ($\Delta\nu_c$) while using a Voigt lineshape profile. The simulated first harmonic of the WM-LIF signal was compared to the first harmonic of the measured WM-LIF signal and the free parameters were varied following a Trust-Region-Reflective Least Squares Algorithm until the simulation converged to a best-fit solution yielding the integrated area of each transition. The ratio of integrated areas was then used to infer the gas temperature following a standard two-color thermometry technique and assuming an equal FQY for each transition. By performing spectral fitting of the WM-LIF signals in the time domain, the spectroscopic parameters of each absorption transition ($A_{\text{int}}, \nu_0, \Delta\nu_c$) could be extracted from the measured WM-LIF signals despite a fluctuating background from the heated jet. By fitting to the first harmonic of the WM-LIF signal the transient background emission is removed and the best fit parameters of the model can be accurately determined.

WM-LIF signals produced from one scan of the QCL and one scan of the TOPO were simulated and fit to measured data simultaneously to provide a time-resolved measurement at the scan rate of the lasers. For each scan, the WM-LIF signals were simulated as follows: (1) the steady-state WM-LIF signal for each transition was calculated as a function of time, (2) the time-dependent WM-LIF signal for each transition was simulated at each time step in the scan, (3) the WM-LIF contributions from each transition were added together, (4) the WM-LIF signal was passed through a digital lock-in filter to determine the first harmonic signal. The steady-state LIF signal for each transition was calculated using Eq. 1, where measured values of the time-varying laser power, $P(t)$, optical frequency, $\nu(t)$, were used to provide a time-domain, steady-state LIF signal. The time-dependent signal from each transition was calculated assuming its value was driven toward the steady-state LIF signal, was proportional to the difference between the time-dependent and steady-state LIF signals, and scaled by the characteristic rate, τ. The time-dependent LIF signal was initially set equal to the steady-state LIF signal, and the forward Euler method was used to calculate the time-dependent LIF signal at each subsequent time step with discrete time resolution defined by the inverse of the data acquisition rate.

The time-dependent LIF signal was then passed through a digital lock-in filter to determine the first harmonic of the WM-LIF signal using Eq. 7.

V. Results

Figure 2 presents the measured WM-LIF signals in the heated jet (left) and corresponding first harmonic from the measurement and best-fit signal (right). The measured WM-LIF signals shows three scans of the QCL and OPO. For each scan the first WM-LIF signal is produced from the excitation via the QCL, and the second WM-LIF signal is produced by excitation with the OPO. The magnitudes of the WM-LIF first harmonic signals are similar despite the significant difference in optical power, due to the differing transition linestrengths. The $1f$ signals were extracted using a digital boxcar filter applied to the measured WM-LIF and the best-fit first harmonic signal was calculated using the frequency domain model. When calculating the first harmonic signal a filter was applied around the modulation frequency which yields a largely background-free and calibration-free measurement.

Figure 3 displays the summary of the temperature measurements in the heated jet.The red dotted line shows the expected trend if the resulting temperature from WM-LIF perfectly matched the thermocouple measurement. For the measurement around 460 K the measurement standard deviation is 1.94 K (0.41%). For the second measurement near 570 K the standard deviation is 2.73 K (0.49%). The final measurement has a standard deviation of 5.01 K (0.82%). The uncertainty bars show one standard deviation from the mean inferred temperature.

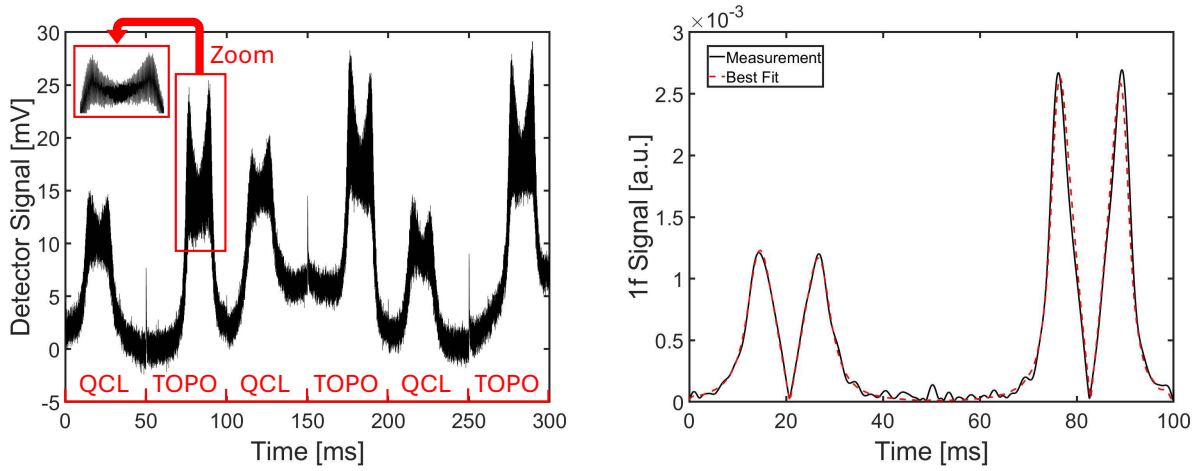

Fig. 2 Raw detector signal measured in a heated jet (left). Corresponding measured and resulting best-fit WM-LIF $1f$ signals for measurements with a laser scan rate of 10 Hz and a modulation frequency of 5 kHz (right).

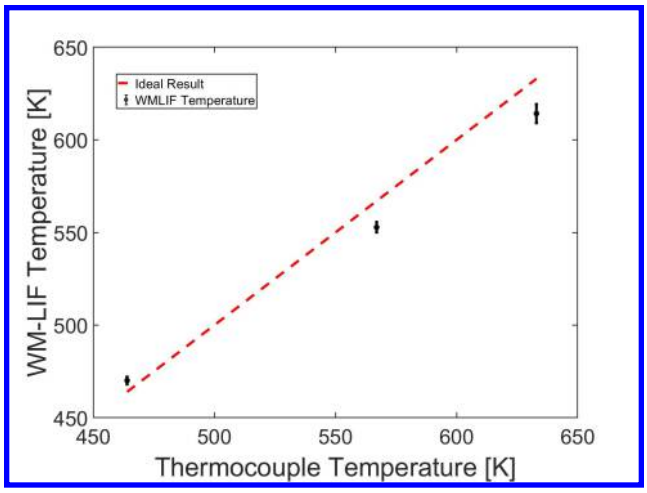

Fig. 3 Comparison between measured jet temperature from a thermocouple and the inferred temperature from WM-LIF.

Figure 4 shows the measured WM-LIF signal and background in the flame (left) and resulting first harmonic from the measurement and best-fit signal (right). The WM-LIF signals are largely hidden within the background emission for the flame. Attempting to model the WM-LIF signal purely in the time domain would be exceedingly difficult due to the low signal-to-background ratio. Instead, modeling the first harmonic signal allows the best-fit parameters to be reliably obtained even with a heavily time-varying background since it varies slowly compared to the modulation frequency.

Figure 5 presents the temperature time history measured in a 49/2/49 $CO/H_2/Ar$ diffusion flame at atmospheric pressure. The $1-\sigma$ measurement precision is 14.0 K (2.47%). Despite the high background emission for the flame, WM-LIF can provide reliable and precise measurements of temperature. The enhancement in precision from wavelength modulation is due to the rejection of the background emission during the filtering process.

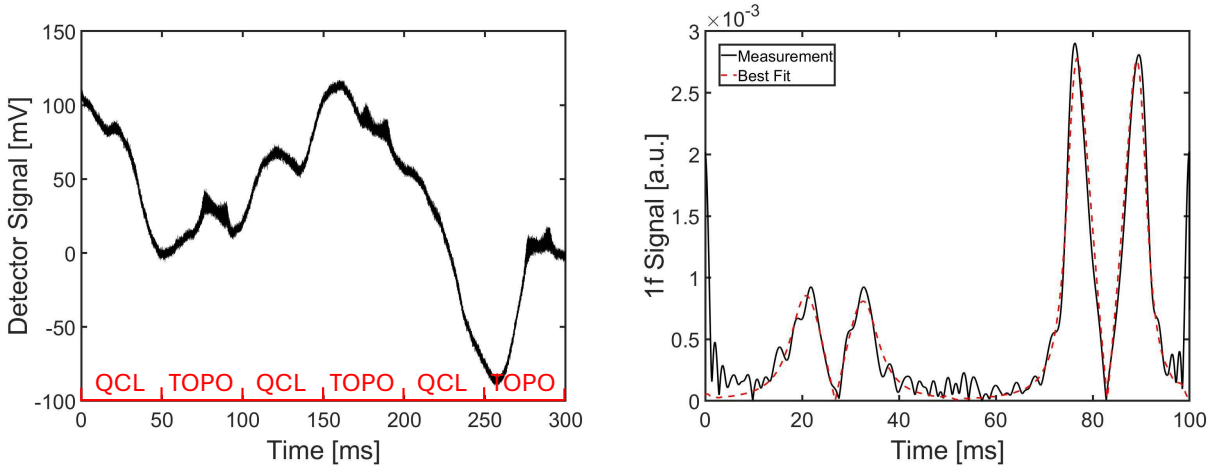

Fig. 4 Raw detector signal acquired in a flame for a condition and measurement location where the LIF signals are small compared to transient background emission from flame gases. Measured and best-fit background-free WM-LIF 1f signals for measurements with a laser scan rate of 10 Hz and a modulation frequency of 5 kHz.

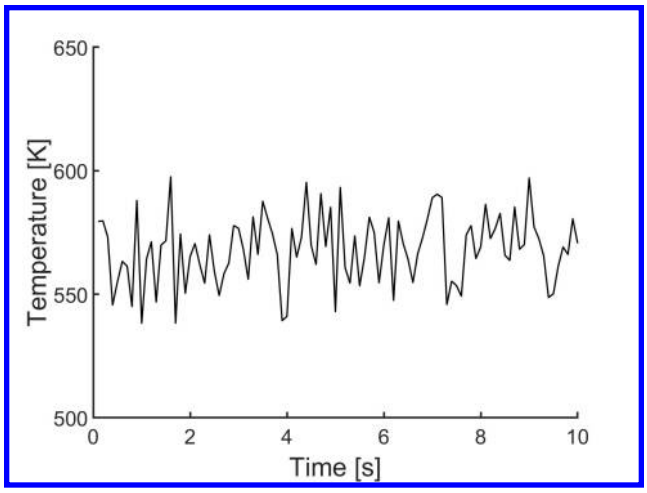

Fig. 5 WM-LIF temperature time history in the core of a 49/2/49 CO/H_2/Ar diffusion flame measured at the centerline with $x/D = 0.167$ above the jet exit.

VI. Conclusions

This work presented the development and initial demonstration of the first two-color wavelength-modulated IR-LIF diagnostic for temperature. Temperature measurements were presented in the core of a diffusion flame and the accuracy of the diagnostic was validated in heated-jet experiments at 460 to 640 K. The WM-LIF temperature measurements exhibit excellent precision (approximately less than 1% of the mean temperature) and agree well with thermocouple measurements. This technique has the potential to yield increased signal-to-noise ratio due to the addition of wavelength modulation as opposed to purely scanned-wavelength LIF techniques. The advancements reported here were achieved by (1) using wavelength modulated LIF and (2) employing novel time and frequency domain LIF models and a spectral-fitting routine to determine spectroscopic parameters and gas properties.

Acknowledgments

This work was supported by NSF CBET CAREER Award 1847464

References

[1] Kirby, B. J., and Hanson, R. K., "Planar laser-induced fluorescence imaging of carbon monoxide using vibrational (infrared) transitions," *Applied Physics B*, Vol. 69, 1999, pp. 505–507.

[2] Kirby, B. J., and Hanson, R. K., "Imaging of CO and CO_2 using infrared planar laser-induced fluorescence," *Proceedings of the Combustion Institute*, Vol. 28, 2000, pp. 253–259.

[3] Kirby, B. J., and Hanson, R. K., "CO_2 imaging with saturated planar laser-induced vibrational fluorescence." *Applied Optics*, Vol. 40, 2001, pp. 6136–6144.

[4] Goldenstein, C. S., Miller, V. A., and Hanson, R. K., "Infrared planar laser-induced fluorescence with a CW quantum-cascade laser for spatially resolved CO_2 and gas properties," *Applied Physics B*, Vol. 120, No. 2, 2015, pp. 185–199.

[5] Mathews, G. C., and Goldenstein, C. S., "Wavelength-modulated planar laser-induced fluorescence for imaging gases," *Optics Letters*, Vol. 42, No. 24, 2017, pp. 5278–5281.

[6] Mathews, G. C., Rustad, J., and Goldenstein, C. S., "Dual-Band Scanned-Wavelength Infrared Laser-Induced-Fluorescence Thermometry of CO," *AIAA SciTech*, , No. 2827, 2024.

[7] Goldenstein, C. S., Strand, C. L., Schultz, I. A., Sun, K., Jeffries, J. B., and Hanson, R. K., "Fitting of calibration-free scanned-wavelength-modulation spectroscopy spectra for determination of gas properties and absorption lineshapes," *Applied Optics*, Vol. 53, 2014, p. 356. doi:10.1364/ao.53.000356.